JOURNAL OF GEOPHYSICAL RESEARCH, VOL. 85, NO. C2, PAGES 1123–1136, FEBRUARY 20, 1980

The Generation of Equatorial Currents

S. G. H. PHILANDER AND R. C. PACANOWSKI

Geophysical Fluid Dynamics Laboratory/NOAA, Princeton University, Princeton, New Jersey 08540

In response to the sudden onset of zonal winds the surface layers of the ocean accelerate in the direction of the wind. Motion is most intense near the equator where a jet forms within a week. The next stage in the evolution of equilibrium conditions is associated with wave fronts, excited initially at the coasts, that propagate across the ocean basin and establish zonal density gradients. Wave modes trapped in and above the strong shallow tropical thermocline because of internal reflection there are responsible for the adjustment of the upper ocean in low latitudes. These thermocline-trapped modes extend over a depth greater than that of the wind-driven surface currents and hence give rise to an undercurrent in the thermocline. This undercurrent is zonal and particularly intense near the equator, where it appears in the wake of an eastward traveling Kelvin or westward traveling Rossby wave after about 1 month. In the case of eastward winds, nonlinearities intensify the eastward equatorial surface jet and weaken the westward undercurrent. In the case of westward winds a different nonlinear mechanisms intensifies the eastward Equatorial Undercurrent and weakens the westward surface flow. In a 5000-km wide basin, equilibrium equatorial currents are established about 150 days after the onset of the winds. The response time of the ocean below a depth of a few hundred meters is much longer. Winds with no spatial and a simple temporal structure generate currents with a complex vertical structure in the deep ocean. Closed current systems are possible in a confined forced region of an unbounded ocean; meridional coasts are not essential for their maintenance. The intensity of equatorial current is sensitive to dissipation parameters.

1. INTRODUCTION

The sudden onset of eastward winds over the eastern part of the equatorial Indian Ocean in the spring and autumn generates intense oceanic jets as shown in Figure 1. The jets at first accelerate, then remain steady even though the winds continue to provide eastward momentum, and after about 10 weeks they suddenly decelerate and reverse direction. What is the explanation for this sequence of events?

The northeast monsoons, which prevail over the Indian Ocean from November until March, are known to generate an eastward Equatorial Undercurrent (see, for example, *Swallow* [1964]. How is an undercurrent generated from a state of rest?

A study of the generation of equatorial currents is clearly of relevance to phenomena in the Indian Ocean. It also contributes to an understanding of variability in the Atlantic and Pacific oceans even though the fluctuations of the winds there are not eventlike but occur over a spectrum of frequencies. The high-frequency response to this forcing will be in the form of waves, but the low-frequency response will correspond to gradual changes in equilibrium conditions [*Philander,* 1976*b*]. An example of low-frequency variability of equilibrium conditions are the El Niño events during which changes in the large-scale density gradients along the equator cause a major redistribution of heat in the equatorial Pacific Ocean. An estimate of the time scale on which equilibrium conditions can change (and Los Niños can occur) is given by the time it takes the ocean to reach equilibrium from an initial state of rest.

The generation of linear currents has been studied in great detail, notably by *Cane and Sarchik* [1976, 1977, 1979], who referenced several earlier studies. These linear solutions are for a constant density ocean with an arbitrary equivalent depth. An appropriate superposition of such solutions describes the flow in a continuously stratified ocean. *Gill* [1975] and, more recently, *McCreary* [1980] make such a superposition in order to study the evolution of the vertical structure of the flow and the generation of the Equatorial Undercurrent.

Paper number 9C1678.
0148-0227/80/009C-1678$01.00

Cane [1979] has investigated the generation of nonlinear equatorial currents by using a numerical model with high horizontal resolution. The vertical resolution, however, is minimal, since the model essentially has two layers.

In this paper we used a multilevel model to study the generation (section 3) of linear and nonlinear equatorial currents in a continuously stratified ocean. Several of the calculations are similar to those of *Cane* [1979]. However, the high vertical resolution of our model (see section 2) permits a relaxation of the troublesome assumption (inherent in a two-level model) that the currents and wave modes have similar vertical structures. (Intense oceanic currents are confined to the upper ocean and have a vertical structure significantly different from that of the first baroclinic mode, which has a node at a depth of about 1500 m.) Other topics that are discussed in this paper include the effects of spatially varying winds (section 5), instabilities (section 6), and the sensitivity of the results to dissipative processes (section 7). Section 8 is a discussion of the principal results.

2. THE MODEL

The equations of motion (the primitive equations) are simplified by making the Boussinesq and hydrostatic approximations and by assuming an equation of state of the form

$$\rho = \rho_0(1 - \alpha T)$$

where ρ is the density, T is the temperature, $\alpha = 0.0002/°C$ is the coefficient of thermal expansion, and $\rho_0 = 1$ gm/cm^3. The coefficients of horizontal ν_H and vertical ν_v eddy viscosity and the thermal diffusivity κ are assumed to have the constant values

$$\nu_v = 10 \text{ cm}^2/\text{s} \qquad \nu_H = 2 \times 10^7 \text{ cm}^2/\text{s}$$

$$\kappa_v = 1 \text{ cm}^2/\text{s} \qquad K_H = 10^7 \text{cm}^2/\text{s}$$

In section 9 we discuss the sensitivity of the results to the values of these parameters. The equations are solved numerically by using the method described by *Bryan* [1969], who discusses the finite differencing schemes in detail.

The model ocean is a rectangular box with a longitudinal

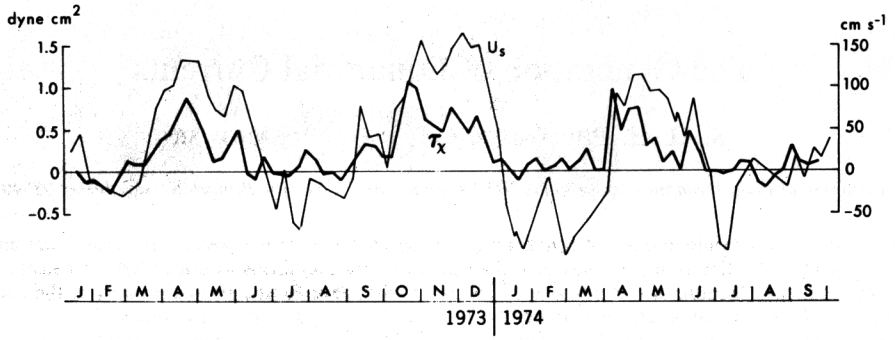

Fig. 1. The zonal velocity component at the surface and the zonal component of the wind stress, as measured on the equator near Gan (70°E) [after *Knox*, 1976].

extent of 4800 km, a latitudinal extent of 2800 km (with the equator in the center), and a depth of 3000 m. In a horizontal plane the 70 × 70 grid points are spaced at regular intervals (of 40 and 70 km in the latitudinal and longitudinal directions, respectively). In the vertical the 16 grid points are spaced irregularly as shown in Figure 4.

Motion is forced at the ocean surface by imposing a wind stress and a condition of zero heat flux:

$$\nu U_z = \tau^x \qquad \nu V_z = 0 \qquad w = 0 \qquad T_z = 0 \text{ at } z = 0$$

At all the other surfaces each of the velocity components and the heat flux are zero. At time t = 0 the wind stress increases from zero for a period of 5 days. Thereafter it has a constant value. This initial sinetaper serves to reduce high-frequency noise.

The initial temperature (and Brunt-Vaisala frequency) is shown in Figure 2. Since ours is a diffusive model, the temperature will immediately start to evolve to a linear profile even in the absence of any forcing. Figure 3 shows this process over a period of 300 days. (There is no motion associated with this diffusive change.) It is clear that the thermocline will appear on a time scale which is long compared to 1000 days. Here, we concern ourselves with transient phenomena which have time scales of a few hundred days at most. We do not address questions concerning the maintenance of the thermocline but confine our attention to the manner in which it is deformed by different forcing functions. Some of the results have been obtained with a linearized version of the model. In such cases the basic stratification is that shown in Figure 2.

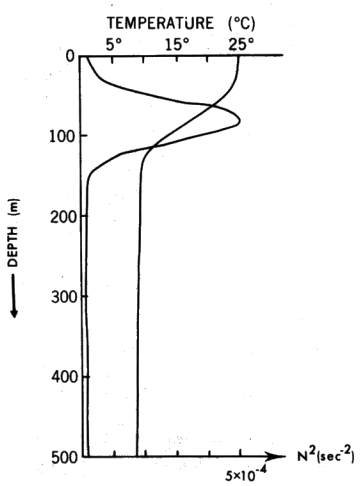

Fig. 2. The initial temperature and Brunt-Vaisala frequency in the upper 500 m of the model. Below 500 m the temperature decreases linearly to zero.

The natural modes of oscillation in the model will play a central role in its adjustment to changes in the surface winds. Figure 4 shows the vertical structure of the first three modes. Their equivalent depths h, gravity wave speeds $c = gh^{1/2}$, radii of deformation $\lambda = c/\beta)^{1/2}$, and time scales $T = (\beta c)^{-1/2}$ are given in Table 1. (The gravitational acceleration is g; β is the latitudinal derivative of the Coriolis parameter f.)

For each of the vertical modes there is a set of latitudinal modes. We shall discuss the low-frequency Kelvin and Rossby modes only and disregard the high-frequency inertia-gravity waves (which are clearly discernible in some of our figures) because they are unimportant in the adjustment of the ocean.

The structure of the second baroclinic mode shown in Figure 4 deserves a comment. In comparison with the other modes this mode is essentially confined to the surface layers. Any disturbance in the surface layers (such as a body force in the upper 50 m) will therefore have a disproportionately large projection onto the second baroclinic mode. In other words, in the adjustment of this ocean to a disturbance in the surface layers the second baroclinic mode will play a dominant role. In Lighthill's [1969] model ocean, on the other hand, the first baroclinic mode is the most important one. The essential difference between the two model oceans is their basic stratifications. Lighthill, in choosing what he thought was a realistic stratification, minimized the importance of the small but finite thickness of the thermocline in the tropics. The importance of this finite thickness is evident in Figure 5, which shows the effect of a typical low-latitude thermocline on downward propagating waves. Note that for certain wavelengths (which correspond to h = 20 and 8 cm, approximately), internal reflection

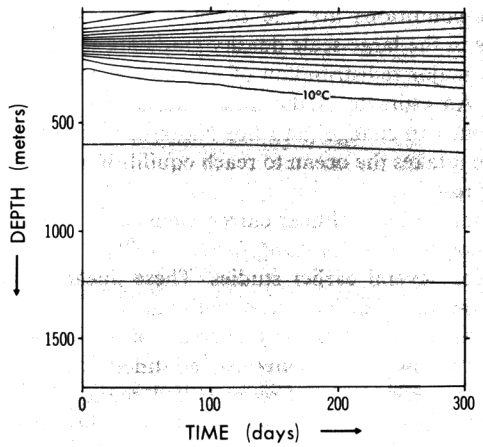

Fig. 3. Diffusive changes in the temperature of Figure 2 over 300 days according to the model. (There is no motion associated with these changes.) Isotherms are at 1°C intervals.

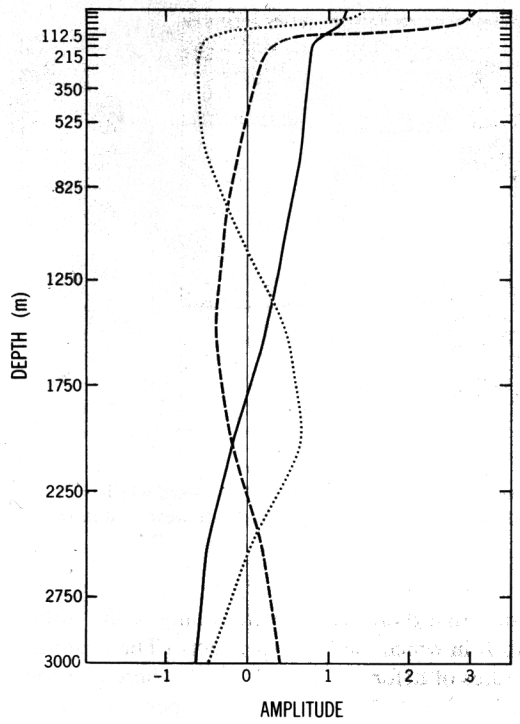

Fig. 4. Structure of the three gravest baroclinic modes associated with the temperature in Figure 2. The vertical resolution of the model is shown in the ordinate.

in the thermocline is so severe that little energy penetrates into the deep ocean. The existence of these wavelengths and, in general, the oscillatory character of Figure 5 are a consequence of the finite depth of the peak of the Brunt-Vaisala frequency N in Figure 2. (In effect, N has two discontinuities, so that the problem is similar to that of light incident on two parallel partial mirrors.) Should we specify that the vertical velocity vanish at the ocean floor and ocean surface, then these boundary conditions are satisfied only for a discrete set of points on the curve in Figure 5. For our stratification the second baroclinic mode practically coincides with the second minimum in Figure 5. Hence this mode has a large amplitude primarily in the surface layers because it is essentially established by internal reflection in the thermocline.

Let us suppose that the ocean is infinitely deep. In that case a discrete set of vertically standing modes are unavailable. Directly wind-driven currents in the surface layers will now generate a spectrum of downward propagating free waves at the coast. Those waves with equivalent depths that correspond to the minima in Figure 5 will be reflected in the thermocline and will form horizontally propagating, leaky modes that are trapped in and above the thermocline. These leaky modes will primarily be responsible for the adjustment of the surface currents to changes in wind conditions. (The radiation of energy into the deep ocean can be viewed as a type of dissipation which is large at the maximum and small at the minima of Figure 5.) The equatorial Atlantic Ocean, where the enormous mid-Atlantic ridge can rise to within 1500 m of the ocean surface, can be regarded as an infinitely deep ocean because the topography will prevent the establishment of the usual vertically standing modes. The leaky modes are then responsible for the adjustment of the upper ocean. This may in fact be the case everywhere in the tropical oceans. The Brunt-Vaisala frequency has a sharp narrow peak throughout the tropics so that the shape of Figure 5 will be nearly the same everywhere. The vertical structure of standing notes, on the other hand, will vary with position because the total depth of the ocean and the depth of the thermocline vary significantly. Hence if we insist on a description in terms of vertical modes, a different combination of these modes will be responsible for the adjustment of the upper ocean in different regions. It is simpler, and may be more accurate, to regard a single leaky mode (at a minimum of Figure 5) as being responsible for the adjustment everywhere. The gravest leaky mode is the most important because its structure coincides closely with that of the wind-driven surface currents. In the model we are using here this leaky mode and the second baroclinic mode are, for practical purposes, the same.

TABLE 1. Scales for Different Vertical Modes

Mode	h, cm	c, cm/s	λ, km	T, days
1	62	250	350	1.5
2	22	145	265	2.1
3	14	115	240	2.3

3. Evolution of the Flow

a. *Linear Response*

Let us briefly review the linear response of a homogeneous, inviscid ocean to the sudden onset of zonal winds that act as a uniform body force throughout the depth h. Such a model is incapable of a realistic simulation of currents. For example, in response to steady zonal winds τ^x the ocean, according to this model, is motionless because the zonal pressure force (due to the slope of the sea surface ζ_x) exactly balances the wind stress:

$$g\zeta_x = \tau^x/h \tag{1}$$

The model is nonetheless of considerable value because an understanding of the evolution of the balance in (1) is essential for the interpretation of results from more sophisticated models.

The balance in (1) evolves in a most fascinating manner. Before the final state of no motion is reached, intense transient currents are generated. Initially, the motion is independent of longitude and the winds drive an accelerating zonal current. There is nothing distinctive about the equator at first, but an equatorial jet of half-width $(c/\beta)^{1/2}$ forms after time

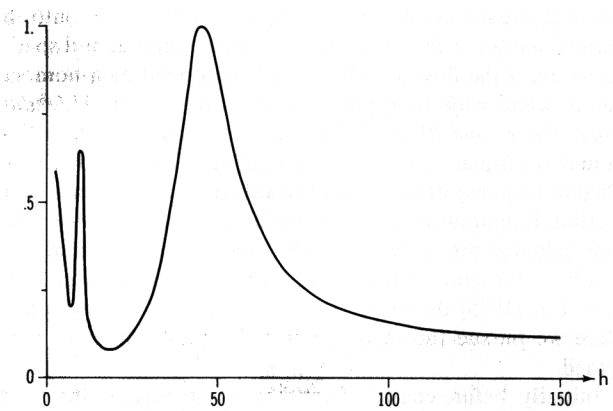

Fig. 5. The ratio of the downward flux of energy at 4000 m to that incident above the thermocline for typical stratification in the tropics as a function of equivalent depth h [after *Philander*, 1978]. (An equation of the type $w_{zz} + (N^2/gh)\, w = 0$ is solved to obtain this curve.)

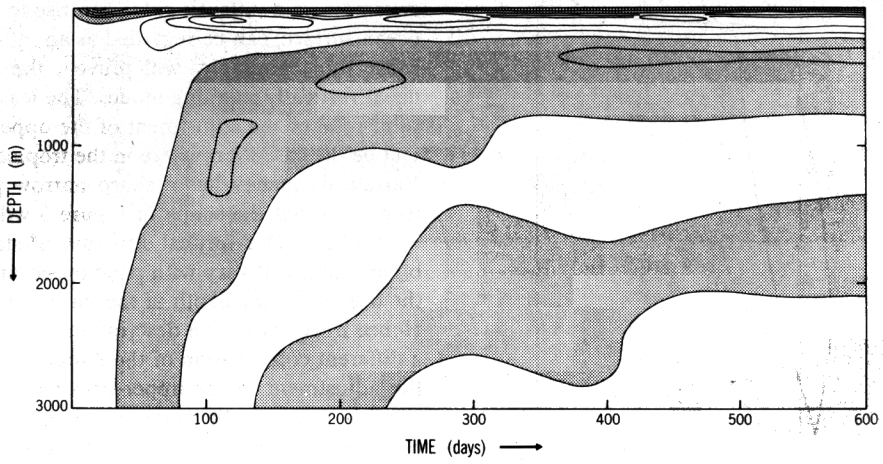

Fig. 6. Evolution of the linear flow at a point on the equator in the center of the basin in response to westward winds with an intensity of 0.5 dyne/cm^2. The zonal velocity contours are at intervals of 20 cm/s. Shaded areas indicate westward flow.

$(\beta c)^{-1/2}$, approximately [*Yoshida,* 1959] (see Table 1 for numerical values). The next stage in the adjustment of the ocean is associated with the propagation of wave fronts excited initially at the coasts. After the passage of a front the acceleration of the equatorial jet stops. This happens because the wave fronts establish a zonal pressure gradient which balances the wind stress. Along the equator the most important wave fronts are the Kelvin from the western coast [D. W. Moore, private communication, 1971; *Gill,* 1975] and the gravest equatorially trapped Rossby waves from the eastern coast [*Cane,* 1979]. The propagation of either front into regions where zonal pressure gradients already exist causes the flow there to decelerate and to become westward. In addition to the waves excited initially, the Rossby wave due to the reflection of the initial Kelvin wave at the eastern coast is important in the adjustment of the ocean [see *Cane,* 1979]. After this wave has crossed the basin (after a time 4T, where T is the time it takes a Kelvin wave and 3T is the time it takes the gravest Rossby wave to cross the basin) there exists a zonal pressure gradient given by (1). By this time the intense jets generated initially have disappeared. Small velocity fluctuations and sea level fluctuations about the mean state will persist in the absence of friction because of repeated wave reflections.

The linear response of a continuously stratified, inviscid ocean driven by a body force in the surface layers can be described in terms of the response of the inviscid, homogeneous ocean discussed above. (The body force is projected onto the vertical modes of the stratified ocean; the temporal and spatial structure of the flow in each mode is described by a homogeneous ocean with an appropriate equivalent depth [*Lighthill,* 1969; *Moore and Philander,* 1977].) Since each of the vertical modes is ultimately motionless, it follows that the final equilibrium response of an inviscid stratified ocean is a state of no motion. Longitudinally sloping isotherms give a pressure force that balances the body force. The evolution to this final state involves transient currents with a complicated vertical structure. *Gill* [1975] describes the early stages of this evolution. Here we pursue the matter until an equilibrium state is attained.

Initially, before coastal effects become important, the winds generate an accelerating equatorial jet which, in the vertical, is confined to the forced region. (This can be inferred from the linear zonal momentum equation at the equator:

$$U_t = \tau^x/D$$

which says that there is acceleration only in the surface layer of depth D in which the body force acts.) The width of this jet is the radius of deformation $(ND/\beta)^{1/2}$, where N is the Brunt-Vaisala frequency of the fluid. It is important to realize that the structure of the jet is independent of the stratification of the deep ocean. In particular, its vertical structure need not bear any resemblance to the structure of vertically standing modes (which depend on the stratification of the entire water column).

The surface equatorial jet can not persist right up to the coasts. To meet the boundary conditions there, the free modes of oscillation of the ocean are excited. The amplitude of a mode is determined by the projection of the latitude-depth structure of the surface jet onto that mode. At the western coast, Kelvin waves and, at the eastern coast, Rossby waves, of the first, second, ···, baroclinic modes, are excited. The arrival of the first baroclinic mode Kelvin wave at a point will introduce a zonal pressure gradient even at depths greater than that of the surface jet because the vertical structures of the mode and jet do not coincide. In response to this pressure force there is a geostrophic meridional flow: an eastward pressure force will give rise to equatorward motion. At the equator the meridional velocity component vanishes by symmetry. As a fluid particle approaches the equator, it tends to move eastward, down the pressure gradient. Hence after arrival of the first wave from a coast a zonal pressure force and, subsequently, an undercurrent (in a direction opposite to that of the surface jet) are established. The arrival of higher baroclinic modes will in turn modify the vertical structure further. Figure 6 is an example of the evolution of the vertical structure in a linear model in response to the sudden onset of westward winds. In an inviscid model these currents are transients; ultimately, there will be no mean currents, as explained above. In a diffusive model the slowly traveling high-order modes could decay rapidly (since they have small spatial scales), and in that case, mean currents will be present in the final equilibrium state. To be quantitative, we have to describe results from the linearized version of our continuously stratified model.

The central panels in Figure 7 show the evolution of the linear flow along the equator in response to the sudden onset of westward winds with a stress of 0.5 dynes/cm^2, as given by

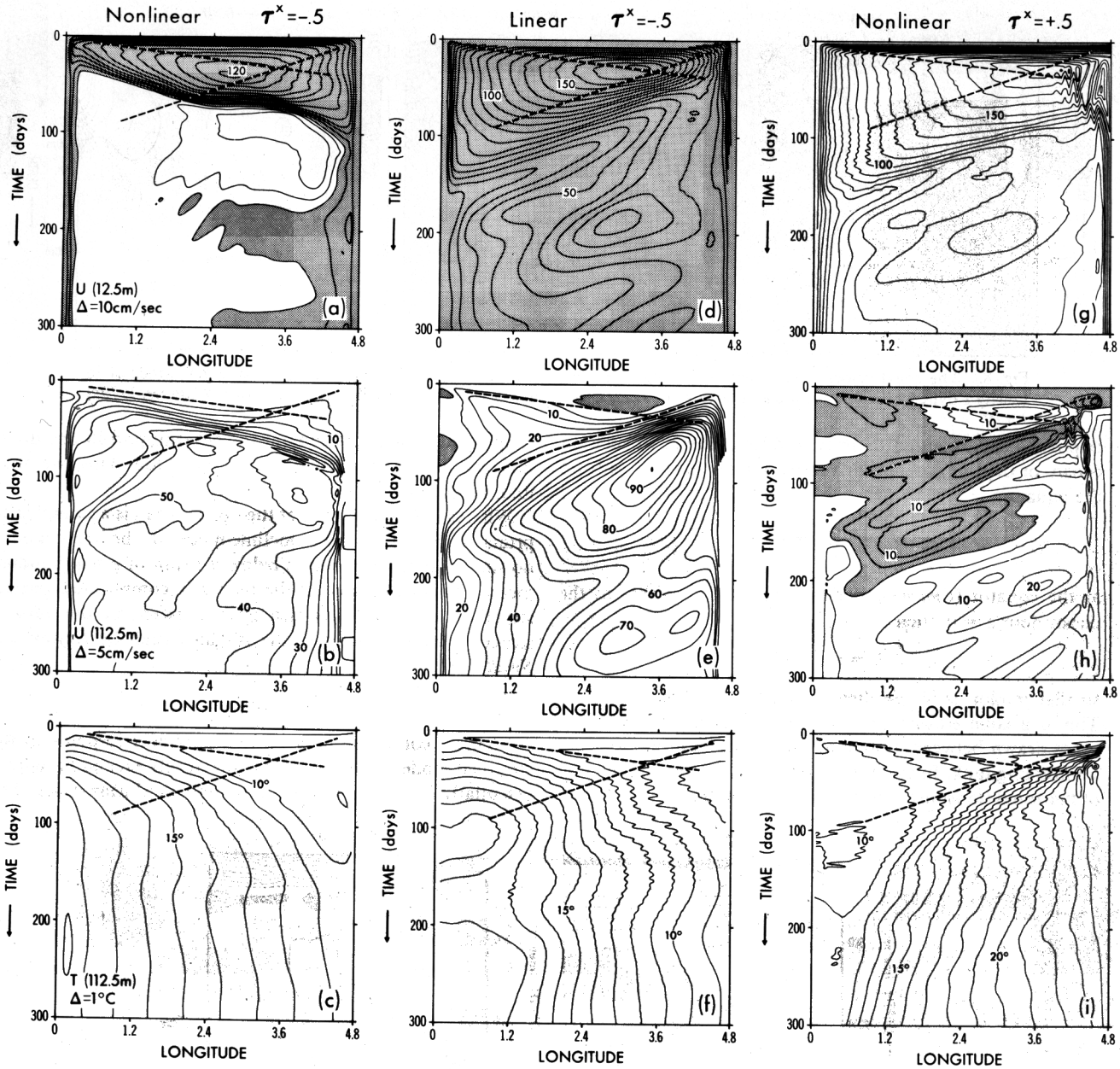

Fig. 7. Evolution of the zonal velocity (at depths of 12.5 and 112.5 m) and temperature (at a depth of 112.5 m) in the equatorial plane. The pair of dashed lines (which is the same in all the plates) corresponds to initially excited Kelvin and nondispersive Rossby waves of the second baroclinic mode. Shaded areas indicate westward flow. Numerical values on contours indicate the velocity in centimeters per second. Longitude is measured in units of 1000 km from the western coast.

our model. Notice that the westward surface jet ceases to accelerate after the arrival of the initially excited Kelvin and Rossby waves. (The dashed lines correspond to the second baroclinic mode Kelvin and nondispersive Rossby waves according to the numbers in Table 1). In section 2 we pointed out that the second baroclinic mode is likely to be more prominent that the other modes. It is, nonetheless, remarkable to what extent this mode is dominant in the adjustment of this ocean. In addition to the waves excited initially, the Rossby wave due to the reflected Kelvin wave is important in the adjustment to equilibrium conditions. After 150 days there basically is an equilibrium state on which small perturbations are superimposed. (Calculations were continued up to day 600 to confirm that this is indeed the case; see, for example, Figure 6.)

The second baroclinic mode, which practically coincides with the gravest leaky mode discussed in section 2, is effectively responsible for the adjustment of the upper layers of this ocean. It has a vertical structure close to but not identical to that of the wind-driven surface currents. This difference accounts for the presence of the eastward Equatorial Undercurrent below the westward surface flow. The persistence of the Undercurrent in this linear model is attributable to friction which attenuates the higher-order baroclinic modes. (These higher modes would have eliminated all the currents, including the undercurrent, in the absence of dissipation, as described earlier.) The width and depth of the undercurrent is simply determined by the scales associated with the dominant baroclinic mode. The stratification is a crucial parameter and is essential for the existence of a linear undercurrent, which is

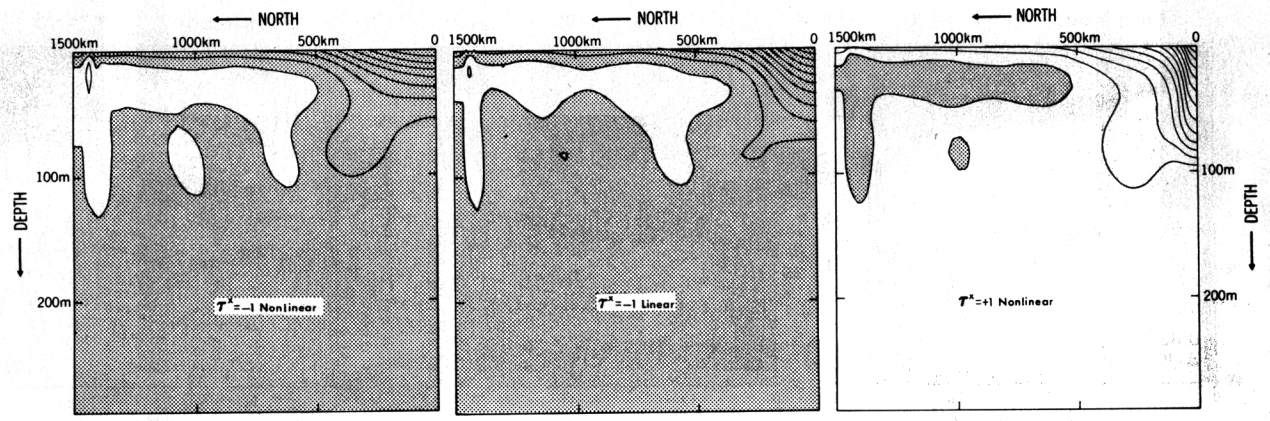

Fig. 8. The zonal velocity component in a longitude-independent model 7.5 days after the onset of zonal winds of intensity 1 dyne/cm^2.Contours are at intervals of 20 cm/s. Westward flow indicated by shaded areas [after *Philander*, 1979*a*].

impossible in a constant density, diffusive ocean. In such an ocean, of depth h, motion driven by a wind stress τ^x satisfies the equation

$$\nu U_{zz} = \frac{1}{\rho_0} P_x = \tau^x / h$$

at the equator [*Charney*, 1960]. Hence if U vanishes at the ocean floor $z = 0$, then

$$U = \tau^x z^2 / 2\nu h$$

so that motion is in the direction of the wind at all depths. This is a counterexample to the false analogy that is sometimes drawn between motion at the equator and motion in a nonrotating tank. In the nonrotating tank the vertical integral of the zonal transport must vanish (if latitudinal variations are suppressed), but at the equator the net transport in one direction can return at a slightly higher latitude. This, we shall find, is indeed what happens.

Whereas the adjustment of the upper ocean is accomplished primarily by the second baroclinic mode (or the leaky mode), no single mode is dominant below a depth of a few hundred meters. This is reflected in the relatively complicated vertical structure of Figure 6, which is reminiscent of the vertical structure measurements in the Indian Ocean by *Luyten and Swallow* [1976].

b. *The Nonlinear Response*

Figure 7 contrasts the linear and nonlinear response of the stratified model. The role of the wavefronts excited initially is essentially the same in the linear and nonlinear cases. The

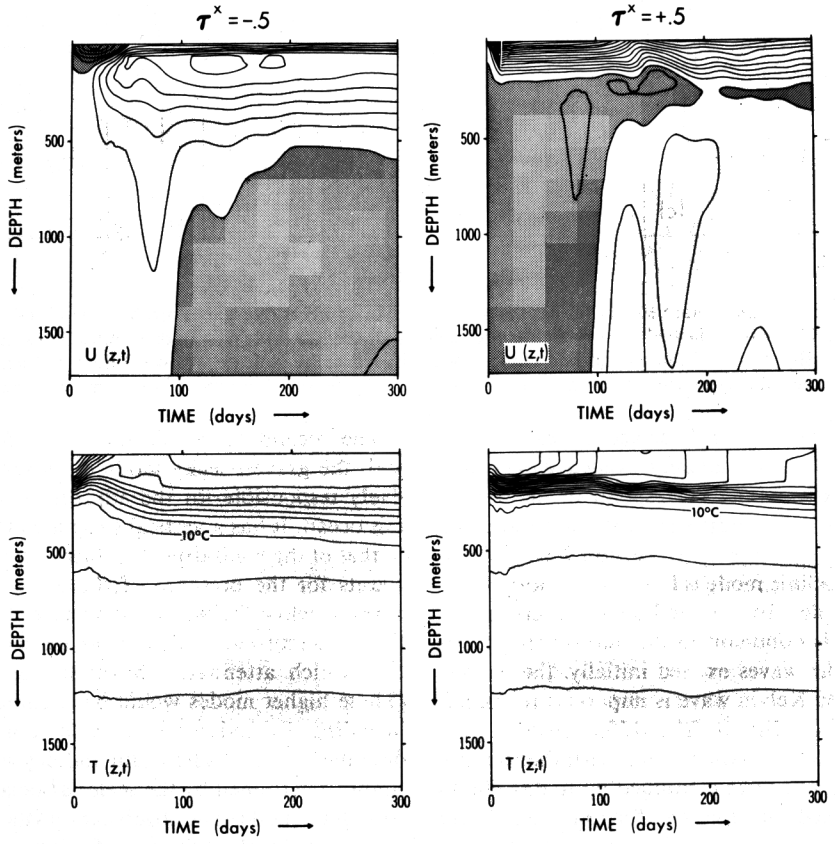

Fig. 9. The zonal velocity component and temperature on the equator at a point in the center of the basin. Isotherms are at intervals of 1°C; contours of zonal velocity are at intervals of 10 cm/s. Shaded areas correspond to westward flow. The results shown are for nonlinear cases.

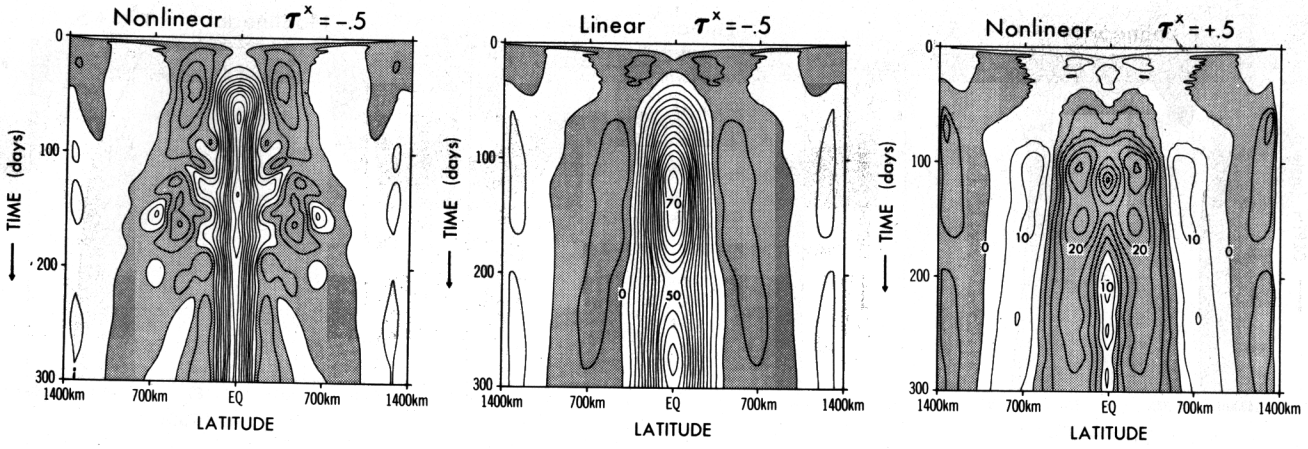

Fig. 10. The zonal velocity component along the central meridian of the basin at a depth of 112.5 m. Contours are at intervals of 5 cm/s.

maximum of the westward surface current is displaced slightly westward, and that of the eastward surface current is displaced slightly eastward by nonlinearities. This suggests that the speed of a wave front is enhanced by currents in its direction and is diminished by opposing currents. Nonlinearities are seen to intensify the eastward surface current and to weaken the westward current. These nonlinear effects are associated with (1) the meridional circulation induced by the surface winds and (2) the meridional circulations induced by the zonal pressure force. We discuss these effects in turn.

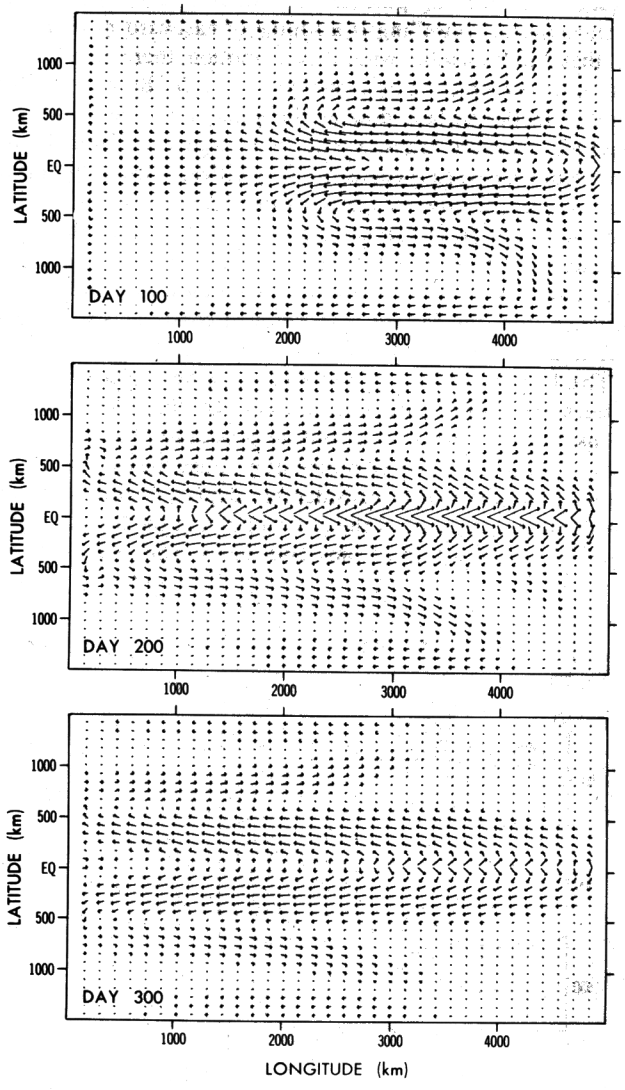

Fig. 11. Instantaneous horizontal velocity vectors in a plane at a depth of 112.5 m. The nonlinear motion is in response to eastward winds with an intensity of 0.5 dyne/cm^2.

Consider longitude-independent flow (without zonal pressure gradients) in response to uniform westward winds. The vertically integrated meridional transport must be zero (because it vanishes at the equator by symmetry). Hence the divergent flow in the surface layers is compensated by convergence at depth and equatorial upwelling. In the surface layers, westward momentum is removed from the equator; it is not replaced at depth. Hence nonlinearities will weaken the westward wind-driven flow [*Gill,* 1975]. The meridional circulation also causes the nonlinear westward jet to be shallower and broader than its linear counterpart. A wind-driven eastward jet will be more intense, narrower, and deeper than a linear jet by similar reasoning. (The equatorward transport of eastward momentum near the surface exceeds the poleward transport of eastward transport at depth in the case of eastward winds.) These effects are demonstrated in Figure 8. Nonlinearities appear to provide a source of eastward momentum at the equator, independent of the direction of the wind, but this statement must be interpreted with caution. It does not imply that an eastward equatorial current can be generated, through nonlinear processes, in response to westward winds when the motion is independent of longitude. Such a phenomenon would be inconsistent with the conservation of angular momentum according to which fluid that arrives at the equator from higher latitudes will move westward.

Should a zonal pressure gradient exist, then angular momentum need not be conserved. Furthermore, zonal variations permit fluid to converge on the equator without there being upwelling or downwelling. The geostrophically induced equatorward flow (in response to an eastward pressure force) could therefore feed an equatorial current whose transport will vary longitudinally. If this equatorward and zonal motion is nondivergent, then the vertical component of the vorticity will be conserved:

$$\beta Y_0 = \beta Y - U_y \rightarrow U = \tfrac{1}{2}\beta(Y - Y_0)^2$$

(Here Y denotes latitude, and Y_0 denotes the original latitude of the particle where it had no zonal momentum.) It follows that as the particle moves equatorward, it acquires eastward momentum [*Fofonoff and Montgomery,* 1955]. Hence nonlinearities can generate an eastward equatorial current in response to westward winds even in a constant density ocean

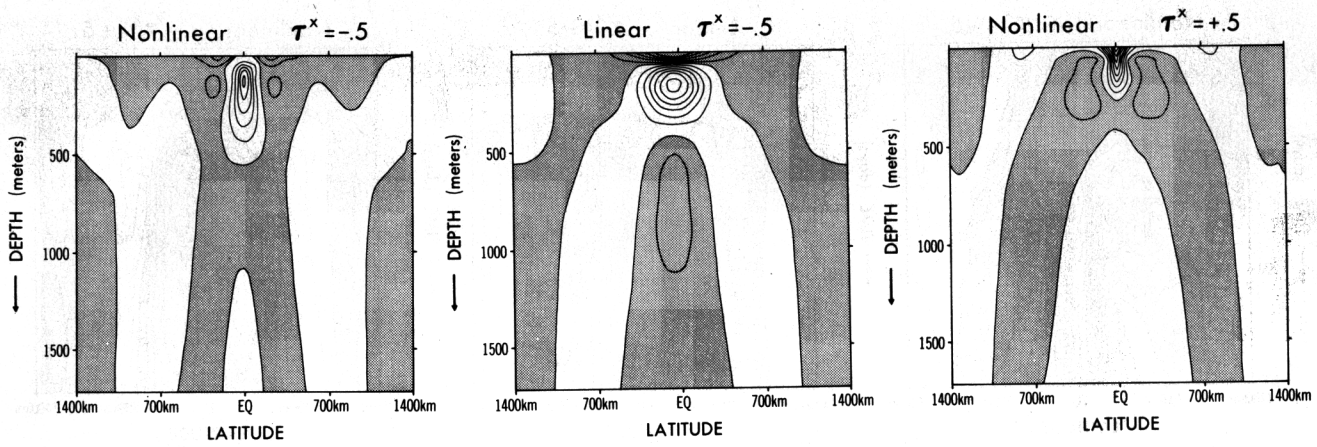

Fig. 12. A section of the zonal velocity component along the central meridian (contours are at intervals of 10 cm/s). The linear case is an instantaneous section at day 300. The nonlinear cases correspond to averaged conditions for the period from day 300 to 350.

[*Charney,* 1960; *Robinson,* 1966]. The existence of an eastward pressure force is necessary for this current to be possible, but as we have seen in section 3*a*, it is not a sufficient condition.

The nonlinear intensification of the eastward surface jet and the weakening of the westward jet in Figure 7 are the consequence of the wind-induced meridional circulation, as explained above. Coastal effects are propagated into the oceanic interior by Kelvin and Rossby wave fronts. As in the linear case, the wave fronts establish zonal density gradients which now balance the wind stress, so that the acceleration of the surface jets ceases once the wave fronts arrive. The propagation of the Kelvin wave is essentially in accord with linear theory, although it is slightly accelerated by the wind-driven eastward jet. The Rossby wave is more significantly retarded by eastward currents. The wind-driven eastward jet prevents the Rossby wave excited initially at the eastern coast from propagating away from that coast (Figure 7*g*). It even retards the reflection of the Kelvin wave (as a Rossby wave) at the eastern coast. Calculations show that for more intense eastward winds the departure of the Rossby wave can be delayed further.

Once a zonal pressure gradient is established, there is a dramatic departure from linear theory for the case of westward winds. (Compare Figures 7*a* and 7*d*, for example.) An eastward pressure force will induce equatorward motion and this will (because of vorticity conservation) tend to intensify the subsurface eastward equatorial current, as described earlier. Close to the equator the vorticity balance is modified by intense upwelling which acts as a sink of eastward momentum at the depth of the thermocline. This offsets the tendency for equatorward moving particles to accelerate eastward. In the surface layers, upwelling is a source of eastward momentum so that the westward wind-driven motion there decelerates and reverses direction as shown in Figure 7*a*. Because of this change in the surface flow at the equator the vertically integrated eastward transport there is large even though the maximum eastward speed is not very different from the linear case. Figure 7*a* and, to a lesser extent, Figure 7*c* show that Rossby waves from the eastern coast also modify the flow signficantly. We shall later show that in its equilibrium state the transport of the undercurrent increases with increasing distance from the eastern (not western) coast. This is in part due to a Rossby wave front.

The linear response to an eastward wind includes a subsurface westward equatorial current. In the nonlinear response this current is weak and deep because the downward diffusion and advection of momentum cause the eastward surface jet to penetrate to considerable depths. Figure 9 shows the nonlinear response at the central point in the basin, on the equator, as a function of time and depth. The arrival of the

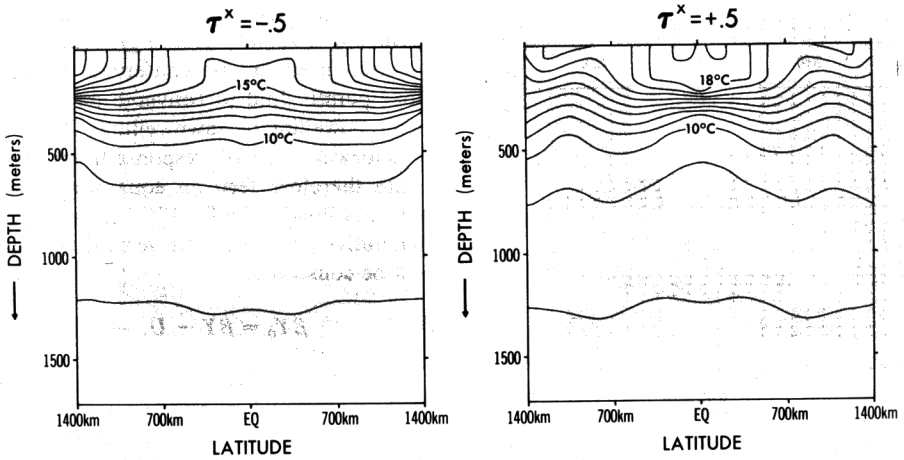

Fig. 13*a*. The temperature sections associated with the nonlinear velocities of Figure 12. The westward wind case is on the left; the eastward wind case is on the right.

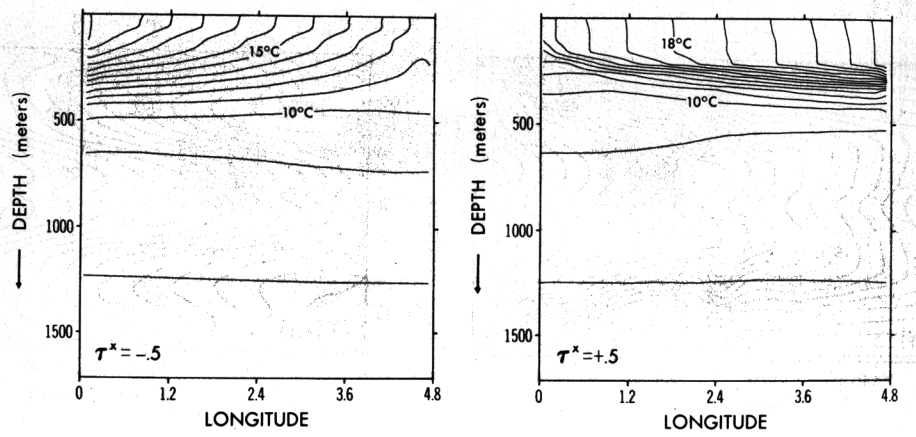

Fig. 13*b*. The temperature in an equatorial plane for the nonlinear cases, as obtained by averaging over the period from day 300 to 350. The westward wind case is on the left; the eastward wind case is on the right. Longitude is measured in units of 10^3 km.

Kelvin wave coincides with the cessation of upwelling (downwelling). The arrival of the Rossby wave is more difficult to discern.

From Figure 10 it is evident that nonlinearities intensify and compress eastward currents but weaken and broaden westward jets.

Motion within about 500 km of the equator evolves to an equilibrium state in about 150 days, which is the time it takes a second baroclinic mode Kelvin wave to propagate eastward across the basin plus the time for the reflected Rossby wave to propagate westward. (Nonlinearities do not modify this time significantly.) Poleward of 5° latitude we expect Ekman drift plus weak geostrophic currents in response to a zonal pressure gradient once the motion is in equilibrium. How is this state approached? Two sets of Rossby waves are excited along the eastern boundary, the first set by the sudden onset of the winds and the second set by the equatorial Kelvin wave that is incident on this coast. The set of Rossby waves is composed of equatorially trapped ones that propagate rapidly but that are confined to the neighborhood of the equator and higher-mode waves that propagate slowly but extend into nonequatorial latitudes. (These higher modes can be viewed as waves radiated by a poleward traveling coastal Kelvin wave [*Moore*, 1968; *Anderson and Rowlands*, 1976]). In the wake of the second set of Rossby waves, equilibrium conditions are established. Figure 11 shows the evolution of these conditions.

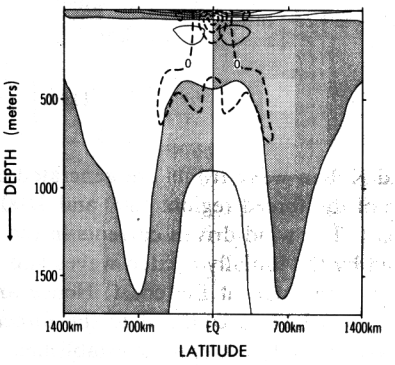

Fig. 14. The meridional circulation in the plane of the central meridian, obtained by averaging the nonlinear results for 50 days from day 300 to 350, for the case of westward winds. Solid contours (at intervals of 5 cm/s) show the meridional velocity component. Shaded areas coincide with southward flow, unshaded areas with northward flow. Dashed contours (at intervals of 0.0015 cm/s) show the vertical velocity. Inside the contour marked 0 there is upwelling.

4. Equilibrium Conditions in Response to Zonal Winds

The equilibrium, nonlinear response to westward winds includes unstable currents (see section 8). We eliminate these and describe here 'mean' conditions, which are obtained by averaging the nonlinear results over the 50-day period from day 300 to day 350. (The period of the instabilities in our model is 25 days.)

The averaged currents along the central meridian of the basin are shown in Figure 12. In the linear case the vertically integrated transport is zero; in the nonlinear cases the net eastward transport at the equator is returned by relatively weak neighboring westward currents. Figure 13 depicts the temperature fields associated with the nonlinear cases. Eastward winds cause convergence and downwelling at the equator, where the isotherms are pinched. The thermocline slopes down toward the east. Westward winds cause upwelling and a spreading of the equatorial thermocline, which slopes down toward the west. The slight downward bowing of some isotherms near the equator in the case of westward winds is an indication of a geostrophic balance rather than downwelling. The meridional circulation in the plane of the central meridian of the basin shows upwelling down to a depth of 500 m near the equator (Figure 14).

Figure 15 shows that the vertically integrated eastward transports near the equator gradually decrease downstream and return westward in the earlier mentioned westward currents which are centered on about 3° latitude. The circuit is closed by a boundary layer on the western coast of the basin. The existence of this boundary layer on the western but not eastern coast and the gradual downstream reduction in transport are attributable to the Rossby waves that emanated from the eastern boundary. As mentioned earlier, the eastward currents can delay and possibly prevent Rossby waves from propagating away from that coast if these jets are sufficiently intense. If the Rossby waves are unable to propagate away from that coast, then the eastward transport could be nondecreasing downstream, and a boundary layer on the eastern coast could feed the westward return currents. This appears to happen in the model of *Semtner and Holland* [1980] which generates a very intense eastward equatorial current.

In the linear case the dimensions of the currents are essentially those associated with the second baroclinic mode (see Table 1). The depth scale is given by the assumed stratification. In the nonlinear case a scale analysis can give a dif-

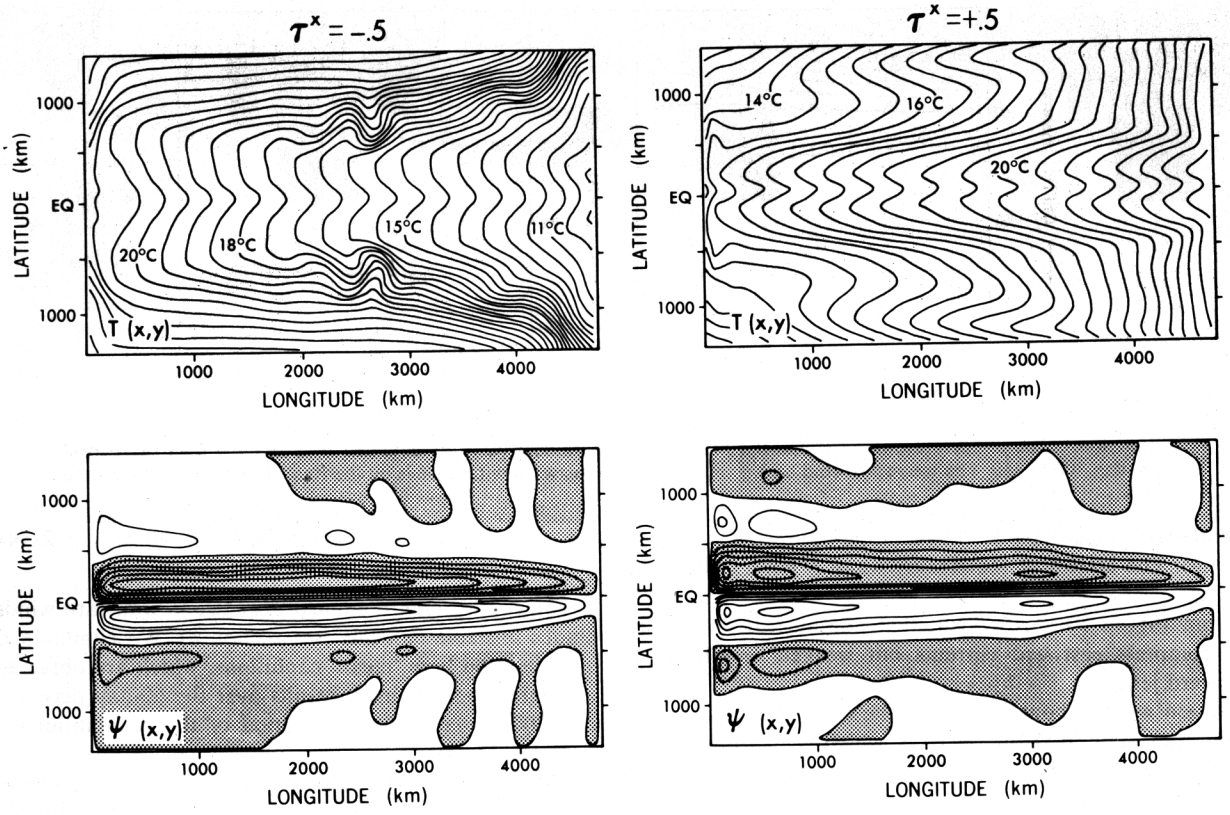

Fig. 15. The temperature at a depth of 12.5 m and the stream function for the vertically integrated transport at day 300 for the nonlinear cases (the contour interval for the stream function is 10^6 m^3/s).

ferent parameter dependence. For example, the width L can be related to the zonal speed U as follows:

$$L \sim (U/\beta)^{1/2}$$

[see *Charney*, 1960]. A scale analysis does not differentiate between eastward and westward currents. Yet we find the scales of these currents to be substantially different (see Figure 8 and 10). The significance of a nonlinear scale analysis is unclear.

The equilibrium conditions described here are not necessarily steady state conditions. On a very long, diffusive time scale the fields could change completely. In the case of eastward winds the downward diffusion of heat and momentum at the equator will continue for much longer than 150 days. The results for eastward winds described here are therefore relevant to transient phenomena with periods up to several hundreds of days (which are less than the diffusive time scale). The nonlinear results for westward winds may be valid for much longer time scales because the downward diffusion of heat and momentum at the equator can be balanced by upwelling.

5. The Effect of Spatially Varying Winds

Thus far we have studied motion with a zonal scale imposed by the size of the basin. In reality, the wind has its own zonal scale which, in the case of the Pacific Ocean especially, is less than the width of the basin. *Cane and Sarachik* [1976, 1977] have studied the response of a linear homogeneous ocean to winds with a spatial structure. We summarize their results for a linear constant density ocean.

Suppose that the ocean, initially at rest, is forced only over a band of meridians between longitude A in the west and B in the east. Outside this strip the wind stress is zero. In the forced region the flow evolves essentially as described earlier. In the unforced region to the east of B, motion is due to Kelvin waves excited initially at A and B and Rossby waves excited at the eastern coast because of reflection of the Kelvin waves. When equilibrium is reached, there is no motion east of the forced region (unless friction is large), but the height of the sea surface has changed by an amount proportional to the distance between A and B. Similar changes occur west of A. We now study the same problem in our nonlinear stratified ocean (see *McCreary* [1980] for the linear solution).

Figures 16 and 17 show the response of the nonlinear model described in section 2 to the sudden onset of zonal winds over a longitudinal strip in the center of the basin

$$\tau^x = \pm H(x) = \pm 0.25 \left[\tanh\left(\frac{x - 1600\ \text{km}}{120\ \text{km}} \right) - \tanh\left(\frac{x - 3200\ \text{km}}{120\ \text{km}} \right) \right]$$

Rossby and Kelvin wave fronts are generated at each of the boundaries of the forced region: 1600 and 3200 km from the western coast. The wind-driven currents in the forced region are modified by the initially excited waves and by waves due to reflections generated at the coast. Hence an equilibrium current system, which is confined to the forced region, still takes approximately 150 days to be established. The structure of the current system is very similar to that described in section 4, but the intensity of the various currents is much reduced (see Figure 17). Horizontal density gradients are confined to the forced region, but the temperature field in the unforced region has been altered because of diffusion and wave propagation. (At a depth of 112.5 m, diffusion tends to

increase the temperature; near the surface it decreases the temperature, as shown in Figure 2.)

The principal result from these calculations is that meridional coasts are not necessary for the generation and maintenance of close current systems. Winds that are confined to a small part of an unbounded ocean can maintain pressure gradients and currents there. Near the equator the region east of the forced area can be permanently influenced by the forcing. This result may shed light on El Niño phenomena: a change in the winds over the western equatorial Pacific only will modify the temperature field in the eastern equatorial Pacific permanently. Hence even if the change in the western part of the basin should occur so gradually that no Kelvin waves are excited explicitly, then there will nonetheless be nearly instantaneous changes in the eastern equatorial Pacific. The seasonal variability in the eastern equatorial Atlantic (Gulf of Guinea) may be related to the seasonally varying winds near equatorial Brazil in this manner because in the equatorial Atlantic, changes on a seasonal time scale seem to occur too slowly for there to be explicit wave excitation. (We have shown here (section 3) that the equilibrium time for an ocean the size of the equatorial Atlantic is about 150 days.)

6. INSTABILITIES

Unstable waves which draw their energy from the mean state appear in a number of our calculations. The westward surface currents adjacent to the Equatorial Undercurrent (in Figure 12) are baroclinically unstable, particularly to distur-

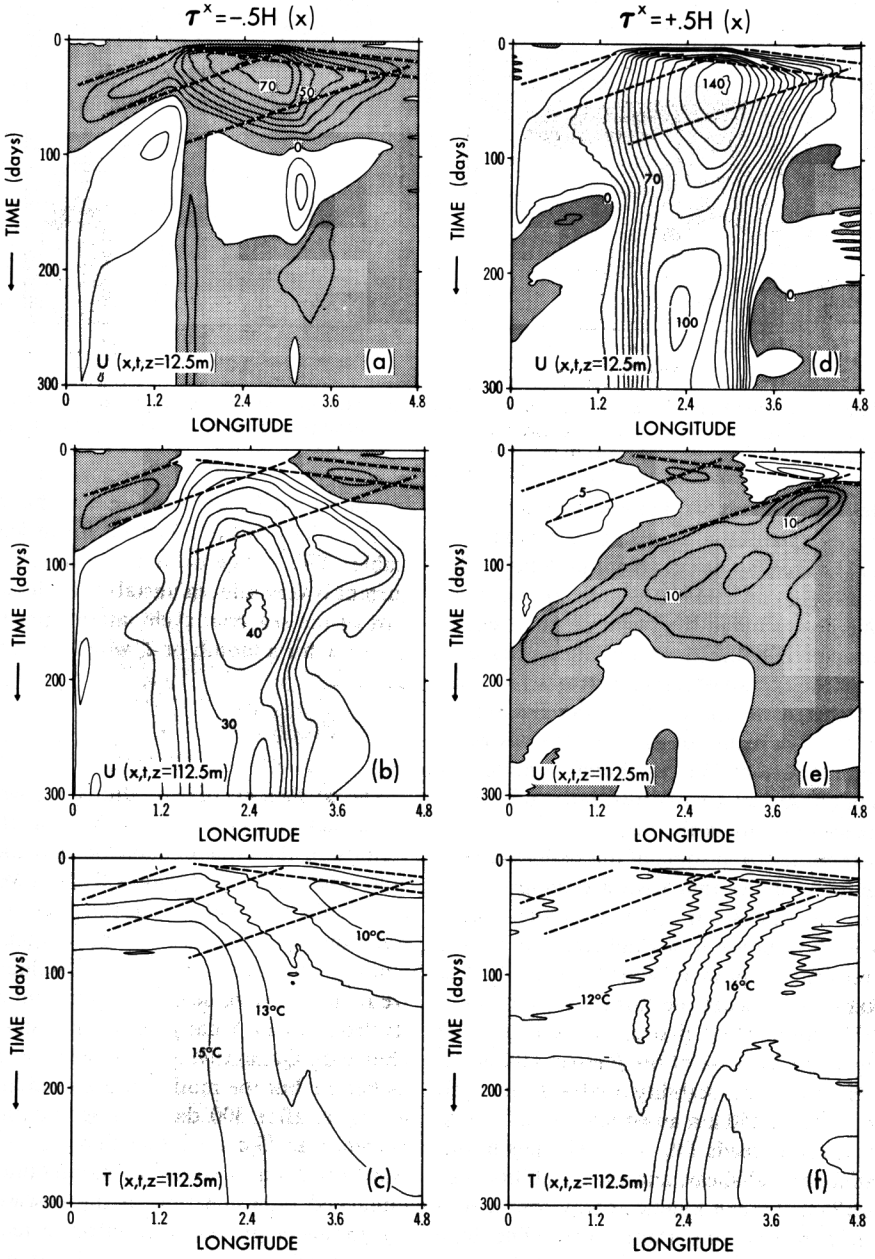

Fig. 16. The evolution of the zonal velocity component and temperature along the equator in response to forcing in the central third portion of the basin. Numbers on contours show the velocity in centimeters per second. Shaded areas coincide with westward flow. The second baroclinic mode Rossby and Kelvin waves (according to Table 1) generated at the edges of the forcing function and the reflection of the first Rossby wave as a Kelvin wave are shown. Longitude is measured in units of 10^3 km.

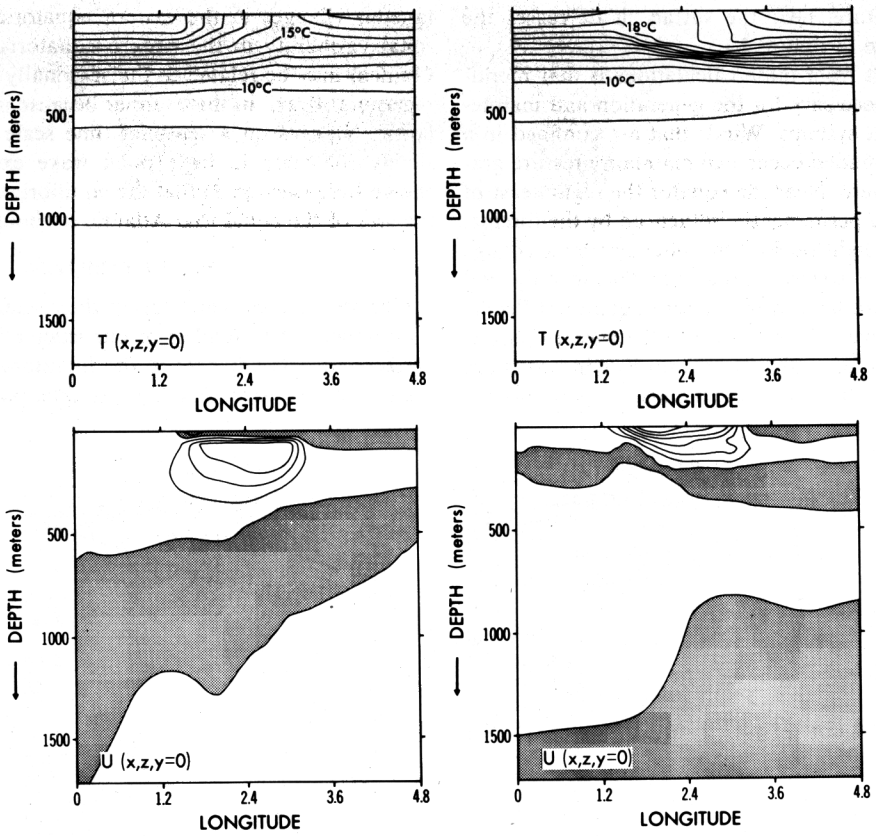

Fig. 17. The density field and zonal currents in the equatorial plane on day 300 in response to westward (left-hand figures) and eastward (right-hand figures) winds that blow over the central third part of the basin. Contours are at intervals of 10 cm/s. Shaded areas indicate westward flow.

bances with a wavelength of about 800 km and a period close to a month. (The same instabilities appear in the model of *Semtner and Holland* [1980], who discuss them in detail.) The mean currents on which the unstable waves grow are not particularly realistic. (We have studied the response of an equatorial ocean to idealized forcing functions and did not have as our goal the realistic simulation of observed currents.) For example, the westward current to the north of the Equatorial Undercurrent in Figure 12 in reality ought to be the eastward North Equatorial Countercurrent. We can therefore not claim that the instabilities in our model are of direct relevance to instabilities that are likely to occur in the ocean.

The absence of instabilities from some of our case studies is also of interest. Figure 7*g* shows that eastward winds of intensity 1/2 dyne generate an eastward jet that attains speeds in excess of 190 cm/s. In response to a wind stress of 1 dyne we found that the maximum speed exceeded 300 cm/s. Yet the jet remained stable even when perturbed with random noise. *Philander* [1976] pointed out that eastward equatorial jets are exceptionally stable because of the β effect and equatorial convergence. His two-layer stability analyses indicated that for a half-width of about 150 km an equatorial jet should be unstable when its speed exceeds 140 cm/s. The jets in our model have substantial vertical shear, and their stability may in part be due to insufficient mean kinetic energy over a suitable depth. There is a second important factor. The high speeds are attained for a period of time which may be short compared to the period of possible unstable waves. In the model of *Semtner and Holland* [1980] the Equatorial Undercurrent in its equilibrium state is sufficiently intense to give rise to unstable waves with a period of about 140 days. Hence in other models, or in the ocean, this current would have to have a speed of 0 (150 cm/s) for at least 140 days to be unstable. This suggests that the observed Equatorial Undercurrent is very seldom unstable. In the central Pacific it can, as part of the seasonal cycle, attain speeds as high as 160 cm/s but only for a month or 2, which is significantly less than 140 days.

7. Sensitivity to Dissipation

The coefficients of eddy diffusivity were arbitrarily assigned the values given in section 2. Various studies of mixing in the vicinity of the equator indicate that these values are reasonable [*Philander and Düing,* 1979]. However, how sensitive are our results to small changes in these values? To answer this question, we repeated the calculation in which a westward wind of intensity 1/2 dyne/cm^2 suddenly starts to blow, but we reduced the value of the coefficient of vertical eddy viscosity from 10 to 5 cm^2/s (all other parameters were left unchanged). Qualitatively, the flow evolved in the same manner as before, but the motion was considerably more intense. For example, after 300 days the maximum speed of the undercurrent was 75 cm/s rather than 52 cm/s. Because the downward diffusion of westward momentum is decreased, there is enhanced intensification of the eastward subsurface current by nonlinear processes. In effect, a reduction in the value of the coefficients of eddy viscosity is equivalent to increased nonlinearity. A calculation in which the intensity of the wind stress was -0.75 dyne/cm^2 and ν_v had a value of 10 cm^2/s gave results qualitatively and quantitatively similar to the case $\tau^x = -0.5$ dynes/cm^2 and $\nu_v = 5$ cm^2/s.

The calculations of *Semtner and Holland* [1980] confirm that the intensity of equatorial currents is very sensitive to the values of the coefficients of eddy viscosity. In their model, $\nu_v = 1.5$, and the effective coefficient of horizontal eddy viscosity is extremely small because a biharmonic formulation is used. They find that a wind stress of -0.5 dyne can generate an eastward equatorial current that at times attains speeds of 160 cm/s!

In order to decide on an appropriate value for the coefficients of eddy viscosity it seems necessary to have simultaneous oceanographic and meteorological data sets. A given model can then be 'tuned' to simulate these data sets.

8. Discussion

In the adjustment of the tropical oceans to changes in the surface winds a mode trapped in the upper ocean is of primary importance. This is a consequence of the stratification in the tropics which is such that the Brunt-Vaisala frequency has high values over a small but nonzero depth range very close to the surface. Because of this stratification, certain leaky modes, the gravest of which coincides with the second baroclinic mode of our model, are established nearly entirely by internal reflection in the thermocline. The vertical structure of this mode therefore closely resembles that of the wind-induced surface currents, so that it plays a primary role in adjustment processes of the upper ocean. No single mode is dominant below a depth of a few hundred meters. Hence the adjustment of the deep ocean is very different from that of the upper ocean (it is much slower, for example). Because of the thermocline-trapped mode the upper ocean is effectively uncoupled from the deep ocean. This implies that the topography of the ocean floor, even features as large as the mid-Atlantic ridge, is unlikely to affect the adjustment of the upper ocean. Measurements in the deep equatorial ocean will be of limited use in the study of the upper ocean.

In our model the thermocline-trapped mode is clearly discernible because of the simple structure of the surface winds which start to blow suddenly. This may be a reasonable approximation to the sudden onset of the westerly winds near Gan in Figure 1. The model suggests that the (highly nonlinear) eastward equatorial jet driven by these winds ceases to accelerate upon the arrival of the leaky mode Kelvin wave excited initially in the west. The deceleration of the jet at a later stage (see Figure 1) could be due to the passage of the Rossby wave front from the east. This wave, however, introduces only weak, subsurface westward flow (Figure 7), whereas the observed westward current is intense at the surface and penetrates to a considerable depth [*Knox*, 1976]. *Cane*'s [1980] suggestion that the reversal of the jet is due to the relaxation of the winds is more plausible.

The vertical structure of the thermocline-trapped leaky mode does not exactly coincide with that of the wind-driven surface currents. It is this discrepancy that gives rise to phenomena such as the subsurface Equatorial Undercurrent. (The usual two-level models cannot simulate these phenomena because the vertical structure of the wind-driven currents in these models coincides with that of the vertical modes. *Cane*'s [1979] model is an exception because the body force is confined to the upper part of the upper layer. Our results with a multilevel model essentially confirm those of Cane.) After the sudden onset of westward winds an Equatorial Undercurrent is established in the wake of a Kelvin wave which takes a month to cross the basin. Nonlinearities then intensify this current (which is maintained by an eastward pressure force) and weaken the westward surface flow when upwelling transfers eastward momentum to the surface. These results suggest that the northeast monsoons prevail sufficiently long to generate an undercurrent in the western equatorial Indian Ocean. This is consistent with the measurements (which are summarized by *Philander* [1973]).

From the oceanic response to a sudden onset of the winds we can make qualitative inferences concerning the variability induced by winds with a complex time dependence. Our results show that an equilibrium equatorial current system is generated after about 150 days. Hence if the wind variations have a longer time scale, then there should be no explicit wave excitation and the response should be an equilibrium one. *Katz et al.* [1977] found this to be the case in the western equatorial Atlantic Ocean: there the zonal slope of the thermocline varies in phase with the seasonal changes in the zonal wind stress. It is important to realize that the topography of the ocean floor in the western equatorial Atlantic is extremely rugged because of the presence of the mid-Atlantic ridge. A vertical mode that depends on reflections from the ocean floor can therefore not be responsible for the rapid adjustment of the ocean which is implied by the result of *Katz et al.* [1977]. We therefore have indirect confirmation of the existence of a thermocline-trapped mode. For a more quantitative test of the model it will be necessary to study the motion induced by more realistic winds. As a next step we intend to study the oceanic response to periodic forcing.

Acknowledgments. It is a pleasure to acknowledge numerous stimulating conversations with M. Cane and E. Sarachik. We are indebted to E. Williams who typed this manuscript and to P. Tunison and his staff who prepared the large number of figures.

References

Anderson, D. L. T., and P. B. Rowlands, The role of inertia-gravity and planetary waves in the response of a tropical ocean to the incidence of an equatorial Kelvin wave on a meridional boundary, *J. Mar. Res., 34,* 295–312, 1976.

Bryan, K., A numerical method for the study of the circulation of the world ocean, *J. Comp. Phys., 4,* 347–376, 1969.

Cane, M., The response of an equatorial ocean to simple wind-stress patterns, Parts I and II, *J. Mar. Res., 37,* 233–299, 1979.

Cane, M., On the dynamics of equatorial currents with application to the Indian Ocean, *Deep Sea Res.,* in press, 1980.

Cane, M., and E. Sarachik, Forced baroclinic ocean motions, I, *J. Mar. Res., 34*(4), 629–665, 1976.

Cane, M., and E. Sarachik, Forced baroclinic ocean motions, II, *J. Mar. Res., 35*(2), 395–432, 1977.

Cane, M., and E. Sarachik, Forced baroclinic ocean motions, III, *J. Mar. Res., 37,* 355–398, 1979.

Charney, J. G., Nonlinear theory of a wind-driven homogeneous layer near the equator, *Deep Sea Res., 6,* 303–310, 1960.

Fofonoff, N. P., and R. B. Montgomery, The Equatorial Undercurrent in the light of the vorticity equation, *Tellus, 7,* 518–521, 1955.

Gill, A. E., Models of equatorial currents, in *Proceedings of the Symposium on Numerical Models of Ocean Circulation,* National Academy of Science, Washington, D. C., 1975.

Katz, E., et al., Zonal pressure gradient along the equatorial Atlantic, *J. Mar. Res., 35*(2), 293–307, 1977.

Knox, R., On a long series of measurements of Indian Ocean equatorial currents near Addu Atoll, *Deep Sea Res., 23,* 211–221, 1976.

Lighthill, M. J., Dynamics response of the Indian Ocean to the onset of the southwest monsoon, *Phil. Trans. Roy. Soc. London, Ser. A, 265,* 45, 1969.

Luyten, J., and J. Swallow, Equatorial undercurrents, *Deep Sea Res., 23,* 1005–1007, 1976.

McCreary, J., A linear stratified ocean model of the Equatorial Undercurrent, submitted to *Phil. Trans. Roy. Soc. London,* 1980.

Moore, D. W., Planetary-gravity waves in an equatorial ocean, Ph.D. thesis, Harvard Univ., Cambridge, Mass., 1968.

Moore, D. W., and S. G. H. Philander, Modeling of the tropical oceanic circulation, in *The Sea,* vol. 6, pp. 319–361, Interscience, New York, 1977.

Philander, S. G. H., Equatorial Undercurrent: Measurements and theories, *Rev. Geophys. Space Phys., 2*(3), 513–570, 1973.

Philander, S. G. H., Instabilities of zonal equatorial currents, 1, *J. Geophys. Res., 81*(21), 3725–3735, 1976.

Philander, S. G. H., Forced oceanic waves, *Rev. Geophys. Space Phys. 16*(1), 15–46, 1978.

Philander, S. G. H., Nonlinear equatorial and coastal jets, *J. Phys. Oceanogr., 9,* 737–747, 1979*a*.

Philander, S. G. H., Variability of the tropical oceans, *Dyn. Oceans Atmos. 3,* 191–208, 1979*b*.

Philander, S. G. H., and W. Düing, The oceanic circulation of the tropical Atlantic and its variability as observed during GATE, *Deep Sea Res., 26* (suppl. II), 1–28, 1979.

Robinson, A. R., An investigation into the wind as the cause of the Equatorial Undercurrent, *J. Mar. Res., 24,* 179–204, 1966.

Semtner, A. J., and W. R. Holland, Numerical simulation of equatorial ocean circulation, submitted to *J. Phys. Oceanogr.,* 1980.

Swallow, J. C., The Equatorial Undercurrent in the western Indian Ocean, *Nature, 204,* 436–437, 1964.

Yoshida, K., A theory of the Cromwell Current and equatorial upwelling, *J. Oceanogr. Soc. Japan, 15,* 154–170, 1959.

(Received June 18, 1979;
revised November 15, 1979;
accepted November 19, 1979.)